

27 **Summary**

28 **Background** We previously found that human identical sequences (HIS) of SARS-CoV-2 promote the
29 clinical progression of COVID-19 by upregulating hyaluronan (HA). As one of the drugs for
30 hyaluronan inhibition, hymecromone was chosen for evaluating its therapeutic effects on COVID-19.

31
32 **Methods** ELISA was performed to detect the level of HA in COVID-19 patients. We first analyzed the
33 correlation between the level of plasma HA and clinical parameters (lymphocytes, C-reactive protein,
34 D-dimer, and fibrinogen). We then assessed the correlation between the plasma HA level and
35 pulmonary lesions, which were quantified by using artificial intelligence based on chest CT scans,
36 including ground-glass opacity (GGO) and consolidation. Furthermore, we assessed the effect of
37 hyaluronan treatment on the formation of pulmonary lesions in mice and evaluated the role of
38 hymecromone on hyaluronan production in cultured cells. Finally, 94 of the 144 confirmed
39 COVID-19 patients received oral hymecromone in addition to standard care, whereas the others with
40 only standard care were treated as control. Abnormal serological markers in two groups were selected
41 to determine the efficacy of hymecromone.

42
43 **Findings** Plasma HA was closely relevant to clinical parameters, including lymphocytes ($n = 158$; $r =$
44 -0.50 ; $P < 0.0001$), CRP ($n = 156$; $r = 0.55$; $P < 0.0001$), D-dimer ($n = 154$; $r = 0.38$; $P < 0.0001$), and
45 fibrinogen ($n = 152$; $r = 0.37$; $P < 0.0001$), as well as the mass ($n = 120$; $r = 0.30$; $P = 0.0008$) and
46 volume ($n = 120$; $r = 0.30$; $P = 0.0009$) of GGO, the mass ($n = 120$; $r = 0.34$; $P = 0.0002$) and volume
47 ($n = 120$; $r = 0.35$; $P < 0.0001$) of consolidation. Mice experiment further verified that hyaluronan
48 could cause pulmonary lesions directly. Hymecromone remarkably reduced HA via downregulating
49 *HAS2/HAS3* expression. Accordingly, the number of lymphocytes recovered more quickly as the fold
50 change of lymphocytes per day was higher in hymecromone-treated patients ($n = 8$) than the control
51 group ($n = 5$) ($P < 0.01$). Moreover, 89% patients with hymecromone treatment had pulmonary lesion
52 absorption while only 42% patients in control group had pulmonary lesion absorption ($P < 0.0001$).

53
54 **Interpretation** Hyaluronan is closely correlated with COVID-19 progression and can serve as a
55 plasma biomarker. As a promising treatment for COVID-19, hymecromone deserves our further
56 efforts to determine its effect in a larger cohort of COVID-19 patients.

57
58 **Funding** National Key R&D Program of China, Major Special Projects of Basic Research of Shanghai
59 Science and Technology Commission, and Shanghai Science and Technology Innovation Action Plan,
60 Medical Innovation Research Special Project, Research of early identification and warning of acute
61 respiratory infectious diseases.

62

63 **Research in context**

64 **Evidence before this study**

65 Our previous study revealed that human identical sequences (HIS) of SARS-CoV-2 promotes
66 hyaluronan production in COVID-19 patients. We searched PubMed for studies associated with
67 hyaluronan and COVID-19 using the search terms (“hyaluronan” OR “hyaluronic acid” OR
68 “hymecromone”) AND (“COVID-19” OR “SARS-CoV-2”) without any language restrictions from
69 inception up to May 27, 2021. The studies showed that hyaluronan was present in lung alveoli of
70 severe COVID-19 and SARS-CoV-2 infection-induced hyaluronan. Meanwhile, one report showed that
71 hyaluronan was related to the severity of COVID-19 based on the research of 32 COVID-19 cases. As
72 the inhibitor of hyaluronan synthesis, hymecromone is already an approved drug for patients with
73 biliary spasms in Europe and Asia. However, it is unclear whether hymecromone is an effective
74 therapeutic drug for COVID-19.

75

76 **Added value of this study**

77 We found significant correlations between hyaluronan and clinical parameters (lymphocytes,
78 C-reaction protein, D-dimer, fibrinogen, and pulmonary lesions) in COVID-19 patients. Hyaluronan is
79 the essential material for the induction of ground-glass opacity formation in the lung of COVID-19
80 patients. The lymphopenia of COVID-19 may be due to T cell exhaustion caused by hyaluronan.
81 Notably, we demonstrated that hymecromone could accelerate the recovery of lymphopenia and
82 pulmonary lesion absorption of COVID-19 in clinical sets.

83

84 **Implications of all the available evidence**

85 Our finding shows that hymecromone could significantly improve the clinical manifestations,
86 especially in severe COVID-19 patients. Reducing hyaluronan using specific drugs could be a
87 promising and alternative therapeutic strategy for COVID-19, especially for the treatment of patients
88 with lymphopenia and pulmonary lesion.

89

90 **Introduction**

91 As of September 17th 2021, more than 226 million infections of COVID-19 have been
92 confirmed worldwide, resulting in approximately 4,666,334 deaths according to the WHO
93 Coronavirus Disease (COVID-19) Dashboard. Significantly, the emergence of B.1.617.2 (Delta)
94 variant has caused breakthrough infections and exacerbated this epidemic¹, which highlights the
95 importance of exploring the common strategy for the treatment of COVID-19 caused by diverse
96 SARS-CoV-2 variants. With such a rapid variation and high mortality of SARS-CoV-2, there is an
97 urgent need for appropriate treatment to prevent the deterioration of moderate and severe COVID-19,
98 and to reduce the mortality.

99 Recently, we identified five identical sequences between the genomes of SARS-CoV-2 and human,
100 termed human identical sequences (HIS), which can promote the accumulation of hyaluronan by
101 activating hyaluronic acid synthase 2 (HAS2)². Accordingly, adult respiratory distress syndrome
102 (ARDS) is one of the typical clinical symptoms in severe COVID-19 patients³, and hyaluronan
103 (hyaluronic acid, HA) is accumulated in the lung of patients with ARDS⁴. Of note, hyaluronan is higher
104 in lung tissue of deceased COVID-19 patients than that in healthy people⁵. Hyaluronan regulates
105 diverse biological and pathological processes involved in inflammation responses, immune responses,
106 and tissue injury⁶. Meanwhile, the other common features of severe COVID-19 patients include
107 inflammatory cytokine storm, lymphocytopenia, and ground-glass opacity (GGO) in the lung^{7,8}.
108 However, the alteration of hyaluronan and its potential role is still unclear.

109 Here, we found hyaluronan was markedly increased in patients with pulmonary lesions and that
110 there is a significant correlation between plasma level of hyaluronan and other clinical parameters in
111 COVID-19 patients, including lymphocytes, C-reactive protein, D-dimer, and fibrinogen. Moreover,
112 we observed that hyaluronan was significantly relevant to pulmonary lesions, including GGO and the
113 consolidation of lung in COVID-19 patients, which further confirmed that hyaluronan directly induced
114 GGO and the consolidation of lung in mice. Notably, we aimed to use the inhibitor of HA synthesis,
115 hymecromone, an approved prescription drug used for treating biliary spasm in Europe and Asia⁹, to
116 evaluate its therapeutic effect for COVID-19.

117

118 **Materials and Methods**

119 **Patient enrollment and experiment animal**

120 All COVID-19 patients enrolled in this study have received a written informed consent upon admission
121 into the Shanghai Public Health Clinical Center (SPHCC), the designated hospital for COVID-19
122 patients in Shanghai, China¹⁰. This study was approved by the Ethics Committee of the SPHCC
123 (YJ-2020-S123-02). COVID-19 for patients was confirmed based on the Guidelines of the Diagnosis
124 and Treatment of New Coronavirus Pneumonia (version 7) published by the National Health
125 Commission of China. Exclusion criteria for COVID-19 patients were listed as below: 1) Serious
126 non-infectious pulmonary diseases, including pulmonary tumor, pulmonary edema, atelectasis,
127 pulmonary embolism, pulmonary eosinophilic infiltration, pulmonary vasculitis etc.; 2) Severe liver
128 and kidney dysfunction: a) ALT and AST value were more than 10 times higher than the upper limit of
129 normal value; b) serum creatinine value was more than 1.5 times higher than the upper limit of normal
130 value; c) total bilirubin was more than 2 times the upper limit of normal value; 3) Patients with biliary
131 obstruction; 4) Pregnant women (urine or serum pregnancy test positive) or lactating women; 5) Other
132 factors considered unsuitable by the researchers for this trial, or the situation that may increase the risk
133 of subjects or interfere with the clinical trial.

134 Adult C57BL/6 mice were purchased from Shanghai Jiesijie experimental animal Co., Ltd
135 (Shanghai, China). All mice were 6–8 weeks of age. Handling of animals was conducted in accordance
136 with the Guide for the Care and Use of Laboratory Animals and were approved by the SPHCC Ethics
137 Committee.

138

139 **Procedures**

140 Laboratory parameters, chest computed tomographic (CT) scans, treatment and outcome data were
141 collected according to the patients' medical records. The mild and severe cases of COVID-19 were
142 distinguished by pulmonary lesions based on chest CT. The mild COVID-19 patients did not have
143 pulmonary lesions, while the severe COVID-19 patients had pulmonary lesions including GGO and/or
144 consolidation. We first detected the plasma hyaluronan levels of COVID-19 patients (n=158) in
145 SPHCC using Enzyme-linked Immunosorbent assay (ELISA) as described previously². Meanwhile,
146 twenty health subjects were recruited to evaluate their plasma hyaluronan levels as the control group.
147 The 48.43 ng/ml of hyaluronan was sensitive to distinguish COVID-19 patients and health subjects via
148 receiver operating characteristic curve (ROC) analysis. Then, we divided the COVID-19 patients into
149 two groups (HA \geq 48.43 ng/ml; HA < 48.43 ng/ml) and confirmed whether there are significant
150 differences between hyaluronan and other clinical parameters (lymphocytes, C-reactive protein,
151 D-dimer, and fibrinogen). The lesion regions in the lungs of COVID-19 patients were quantified by
152 artificial intelligence (AI) as previous description^{11,12}. Furthermore, we analyzed the correlation
153 between hyaluronan and these clinical parameters.

154 Adult male mice were used to assess the impact of hyaluronan on the lung lesions, such as GGO
155 and consolidation. The 200 to 400 kDa of hyaluronan dissolved in 1×PBS was intratracheal to mice (60
156 mg/kg), while the 1×PBS treatment was as the control group. Then, the formation of lung lesions in
157 two groups were monitored via QuantumGX microCT on day four.

158 Moreover, we evaluated whether hyaluronan can reduce hyaluronan levels in the cell using
159 HEK293T and HUVEC cells. Twenty-four hours after HEK293T and HUVEC were treated with
160 DMSO or hyaluronan (250 μ g/ml), cell culture mediums were collected to detect the hyaluronan
161 levels using the Hyaluronan DuoSet ELISA (R&D Systems) according to the manufacturer's
162 descriptions. Meanwhile, we extracted the total RNA of HEK293T and HUVEC cells treated with
163 DMSO or hyaluronan. As previously described in our study², quantitative RT-PCR (RT-qPCR) was
164 performed to evaluate whether hyaluronan can decrease the expression of *HAS1*, *HAS2*, and *HAS3*
165 (*HAS1/2/3*), which are the known hyaluronic acid synthases. The expression of *GAPDH* served as the
166 normalized endogenous control. Relative mRNA expression was calculated via the $2^{-\Delta\Delta C_t}$ method (The
167 primers are shown in Supplementary Table 1).

168 Finally, 144 COVID-19 patients were recruited to assess whether hyaluronan could improve
169 the clinical parameters of COVID-19. Among these patients, 94 patients were oral hyaluronan
170 administration (2 tablets, 0.2 g/tablet, three times a day, before meals) combined with conventional
171 treatment as the experimental group. The other 50 patients only underwent conventional treatment as
172 the control group. Administration of hyaluronan continued until the patients recovered from
173 COVID-19. Chest CT scans, lymphocyte counts, C-reactive protein (CRP), D-dimer, fibrinogen, and
174 plasma hyaluronan were critical clinical indicators during COVID-19 patient treatment.

175

176 **Outcomes**

177 Outcomes of COVID-19 patients were assessed based on the clinical indicators and chest CT images.

178 The primary outcomes were the changes in lymphocyte counts, CRP, fibrinogen, and D-dimer in
179 patients. The secondary outcome was the change in the patients' chest CT results. We also monitored
180 the suspected serious adverse reactions in accordance with regulatory requirements.

181

182 **Statistical analysis**

183 The COVID-19 patients with pulmonary lesions were defined as severe while the others were
184 considered mild. Twenty health subjects without any clinical symptoms were defined as the normal
185 group. Samples (n=158) were collected to compare the levels of hyaluronan in these three groups using
186 the Mann–Whitney test. ROC analysis was used to identify the hyaluronan concentration for
187 distinguishing normal groups and COVID-19 patients. Based on this analysis, COVID-19 patients were
188 divided into two groups ($HA \geq 48.43$ ng/ml; $HA < 48.43$ ng/ml). The significant differences between
189 typical clinical indicators (such as lymphocytes, C-reactive protein, D-dimer, and fibrinogen) in these
190 two groups were calculated by the Mann–Whitney test. Two-tailed Spearman's correlation analysis was
191 performed to evaluate the correlation between hyaluronan and these clinical indicators. Unpaired T test
192 was used to confirm the significant differences between hyaluronan and *HAS1/2/3* expression among
193 hymecromone-treated cells and DMSO-treated cells.

194 In addition, 144 COVID-19 patients were recruited to assess the effect of hymecromone for
195 COVID-19. We further analyzed the effect of hymecromone using these patients with abnormal clinical
196 parameters, including lymphocytes, C-reactive protein, D-dimer, and fibrinogen. For the primary
197 outcomes, we calculated the fold changes of these clinical parameters per day in the
198 hymecromone-treated group and control group and compared the clinical significances using the
199 Mann–Whitney test. For the secondary outcome of change in chest CT results, we compared the
200 hymecromone-treatment group and the control group, including the patients with GGO. According to
201 CT quantitative analysis, we evaluated the change of pulmonary lesions, including improvement and
202 exacerbation in COVID-19 patients classified by different hospitalization days ($X < 14$ day; $14 \text{ day} \leq X$
203 < 28 day; $28 \text{ day} \leq X < 35$ day; X represents the hospitalization days). We calculated the percentage of
204 improvement and exacerbation in different groups and analyzed the significance between the
205 hymecromone-treated group and the control group using Fisher's exact tests. The *P* value less than 0.05
206 was statistically significant (*, $P < 0.05$; **, $P < 0.01$; ***, $P < 0.001$; ****, $P < 0.0001$; ns, not
207 significant).

208

209 **Role of the funding source**

210 The funders of this study had no role in study design, data collection, data analysis, data interpretation,
211 or writing of the report. The corresponding authors had full access to all the data in the study and had
212 final decision-making power to submit for publication.

213

214 **Results**

215 **Hyaluronan is a considerable biomarker to predict COVID-19 progression**

216 A total of 158 COVID-19 patients in SPHCC were conducted to investigate the potential relationship
217 between hyaluronan and the typical clinical indicators for COVID-19. Specifically, 18% (28 of 158)
218 patients without pulmonary lesions were mild, while the other patients (130 of 158) with pulmonary
219 lesions including GGO and consolidation were severe. The plasma HA level showed no significant
220 difference between healthy subjects and mild COVID-19 patients, while the plasma HA level in severe
221 COVID-19 patients were significantly higher than that in the other two groups (figure 1A), indicating
222 there is a potential relation between hyaluronan and pulmonary lesions. Further ROC analysis
223 identified that the 48.43 ng/ml of hyaluronan was sensitive for distinguishing COVID-19 patients and
224 healthy subjects (figure 1B). Then, 158 COVID-19 patients were divided into low HA group (HA <
225 48.43 ng/ml) and high HA group (HA \geq 48.43 ng/ml).

226 Lymphopenia is one of the typical clinical symptoms in severe COVID-19 patients¹³. It is reported
227 that hyaluronan can result in the death of the activated T cell¹⁴. Here, we found that lymphocytes
228 were markedly decreased in the high HA group of COVID-19 patients (figure 1C). As shown in figure
229 1D, hyaluronan was negatively correlated with lymphocytes (n = 158; $r = -0.50$; $P < 0.0001$). The
230 subsets of T lymphocytes, CD4+ T cells, CD8+ T cells, and CD45+ T cells were also significantly
231 reduced in COVID-19 patients with high HA (supplemental figure 1A-C). Similarly, hyaluronan was
232 negatively correlated with the CD4+ T cells (n = 151; $r = -0.44$; $P < 0.0001$), CD8+ T cells (n = 151; r
233 = -0.53 ; $P < 0.0001$), and CD45+ T cells (n = 151; $r = -0.49$; $P < 0.0001$) (supplemental figures 1D-F).

234 Inflammation is another common clinical symptom involved in COVID-19 patients, usually
235 assessed via CRP. Noteworthy, low molecular weight of hyaluronan is an important inflammation
236 mediator.⁶ Surprisingly, we found that CRP markedly increased in the high HA group (figure 2A) and
237 was positively correlated with hyaluronan (n = 156; $r = 0.55$; $P < 0.0001$) (figure 2B). Recent studies
238 revealed abnormal blood coagulation in COVID-19 patients⁷. Clinically, D-dimer and fibrinogen are
239 commonly used to assess a patient's blood coagulation. We found that both were higher in COVID-19
240 patients with high HA and were positively correlated with hyaluronan (figures 2C-F).

241 Collectively, these results reveal that the increase of hyaluronan is significantly relevant to the
242 reduction of lymphocytes and the upregulation of CRP, D-dimer, and fibrinogen in COVID-19 patients,
243 suggesting hyaluronan may play a key role during the clinical progression of COVID-19.

244

245 **Hyaluronan is fundamental for ground-glass opacity formation in the lung of COVID-19 patients**

246 It is well-known that ground-glass opacity of lungs is the other typical clinical manifestation of
247 COVID-19 patients¹⁵, which can develop into consolidation. We quantified the mass and volume of the
248 lung lesion regions involved in GGO and consolidation in 120 COVID-19 patients using
249 uAI-Discover-NCP (beta version). In general, GGO was defined in a range from -750 HU to -300
250 HU, and the consolidation region was defined from -300 HU to 50 HU¹⁶. Notably, hyaluronan was
251 positively correlated with the mass (n = 120; $r = 0.30$; $P = 0.0008$) and volume (n = 120; $r = 0.30$; $P =$
252 0.0009) of GGO, which was also the case in consolidation (supplemental figure 2). A typical case for
253 this correlation is shown in figure 3. The plasma HA levels, GGO, and consolidation clearly increased
254 on the fourth day, compared to the first day (figures 3A-C), indicating the mass and volume of
255 pulmonary lesions (GGO and consolidation) increased along with the upregulation of hyaluronan. CT
256 images further showed the exacerbation of pulmonary lesions, including GGO and consolidation in this
257 patient on the fourth day instead of the first day (figure 3D). Recent research found that there is

258 jelly-like liquid in the lung of COVID-19 patients³. Given that hyaluronan can absorb water reaching
259 1000 times its molecular weight¹⁷, we hypothesize that hyaluronan may be one of the determinants for
260 GGO of lung in COVID-19 patients.

261 To confirm our hypothesis, we delivered hyaluronan intratracheally to the lung in male mice.
262 Significantly, CT images showed that GGO and consolidation of lung occurred in mice treated with
263 hyaluronan while there were no pulmonary lesions in mice treated with $1 \times$ PBS (figure 4). Therefore,
264 these findings supported that hyaluronan acts as a critical material for the formation of GGO and
265 consolidation of the lung in COVID-19 patients, indicating that inhibition of HA synthesis may be a
266 promising strategy for relieving pulmonary lesions in COVID-19 patients.

267

268 **Hymecromone significantly decreases hyaluronan by downregulating *HAS2/HA3***

269 Based on these findings, we realized that reduction of HA production could be an alternative
270 therapeutic strategy for COVID-19, especially for patients with pulmonary lesions. As a derivative of
271 coumarin, 4-MU was shown to inhibit the production of HA¹⁸. Fortunately, we noticed there is a
272 commercial drug, 4-MU, also called hymecromone, which is an approved prescription drugs in China,
273 USA and Europe, even acting as over the counter drugs in some areas. We first verified the inhibitory
274 effect of hymecromone on HA production in HEK293T and HUVEC cells. As expected, HA from
275 culture medium in HEK293T and HUVEC cells treated with hymecromone (250 μ g/ml) were
276 significantly lower than that in DMSO-treated cells (figure 5A). There are three known hyaluronic acid
277 synthases, including *HAS1*, *HAS2*, and *HAS3* (*HAS1/2/3*). As shown in figures 5B-C, hymecromone
278 treatment remarkably downregulated the expression of *HAS2/HAS3*, but did not affect the expression of
279 *HAS1* in HEK293T and HUVEC cells (figures 5B-C). Therefore, hymecromone inhibits the production
280 of hyaluronan by decreasing *HAS2/HA3* expression.

281

282 **Hymecromone accelerates the recovery of clinical manifestations in COVID-19 patients**

283 To further assess whether hymecromone is efficient in improving the clinical parameters of
284 COVID-19, we recruited 144 confirmed COVID-19 patients. Among these patients, 94 (65%) patients
285 with hymecromone treatment were in the clinical trial group, while 50 (35%) patients with support
286 treatment were in the control group (figure 6A). Given the significant correlation between hyaluronan
287 and clinical indicators, we set changes in lymphocytes, CRP, fibrinogen, and D-dimer as the primary
288 endpoints, and the change in chest CT results as the secondary endpoint. To objectively evaluate the
289 effect of hymecromone on COVID-19, we selected COVID-19 patients with abnormal clinical
290 indicators in these two groups. Specifically, there were 5 patients with decreased lymphocytes, 4
291 patients with increased CRP, 7 patients with increased fibrinogen, and 8 patients with increased
292 D-dimer in the control group. In the clinical trial group, there were 8 patients with decreased
293 lymphocytes, 5 patients with increased CRP, 7 patients with increased fibrinogen, and 6 patients with
294 increased D-dimer (figure 6B).

295 Firstly, we focused on the change of pulmonary lesions in COVID-19 patients during
296 hymecromone treatment. We determined the situation of pulmonary lesions, including GGO and
297 consolidation based on CT quantitative analysis. Surprisingly, all the patients with hospitalization days
298 < 14 day had improved pulmonary lesions after hymecromone treatment (figure 7A). The percentage of
299 pulmonary lesion improvement in patients with hymecromone treatment were significantly higher than
300 that in control group ($P = 0.0002$). For the patients with hospitalization between 28 to 35 days, the
301 percentage of pulmonary lesion improvement rate was 86% (6 of 7) patients in the trial group, and 45%

302 (2 of 9) in the control group, respectively. In total, 89% (41 of 46) patients with hymecromone
303 treatment had pulmonary lesion absorption, while only 42% (42 of 100) in the control group had
304 pulmonary lesion absorption ($P < 0.0001$). Different regions of pulmonary lesions in typical cases in
305 two groups were gradually absorbed (figure 7B). As such, patients have better improvement of
306 pulmonary lesions after hymecromone treatment. Thus, hymecromone could promote the pulmonary
307 lesion absorption of COVID-19.

308 Then, we calculated and compared the fold changes of these various clinical indicators per day in
309 these two groups with lymphopenia, CRP elevation, fibrinogen elevation, and D-dimer elevation,
310 respectively. As shown in figure 8A, the fold change of lymphocytes per day was remarkably higher in
311 hymecromone-treated patients, compared to the control group. Similarly, the fold changes of CRP or
312 fibrinogen in hymecromone-treated patients were higher than that in the control group (supplemental
313 figures 3-5). These results implied that hymecromone contributes to the improvement of clinical
314 parameters of COVID-19. Moreover, the fold change of D-dimer tended to be improved, but it is not
315 significant between control group and clinical trial group, which may be due to the limited number
316 of patients.

317 These findings demonstrated that hymecromone is a promising drug for effectively improving the
318 clinical manifestations of COVID-19.

319

320 Discussion

321 Our previous study has found that human identical sequences (HIS) of SARS-CoV-2 could promote
322 hyaluronan upregulation by NamiRNA-Enhancer network during the progression of COVID-19²,
323 indicating that reduction in hyaluronan may be an alternative therapeutic strategy for COVID-19,
324 which is supported by the other reports found that hyaluronan was increased in severe COVID-19
325 patients^{5,19,20}. As an inhibitor of HA synthesis, hymecromone is an approved drug for biliary spasms
326 treatment. Here, we aimed to assess whether hymecromone could promote the prognosis of COVID-19.

327 Hyaluronan is an excellent biomarker to predict COVID-19 progression. We found that
328 hyaluronan was significantly elevated in severe COVID-19 patients. Consistent with our results,
329 increases in hyaluronan was also confirmed in severe or critical patients with COVID-19²⁰. Notably,
330 hyaluronan is accumulated in the bronchoalveolar lavage fluid (BALF) and serum samples of patients
331 with ARDS²¹, a relatively serious COVID-19. We also found that hyaluronan was significantly
332 correlated with lymphocytes, CRP, D-dimer, and fibrinogen. These clinical indicators are proven
333 biomarkers for the clinical progression of COVID-19²². All these findings demonstrated that
334 hyaluronan was relevant to COVID-19 progression. Additionally, we showed that hyaluronan
335 positively correlates with quantified chest CT results, a recently identified parameter to predict the
336 severity of COVID-19¹¹. This result further supported that hyaluronan can serve as a better biomarker
337 for predicting the clinical progression of COVID-19.

338 Most importantly, our results provide vital insights into the typical clinical symptoms occurring in
339 COVID-19. As we all know, GGO is one of typical CT manifestations of COVID-19 patients²³.
340 However, the pathophysiologic mechanism of GGO is still unclear. We showed that hyaluronan can
341 cause GGO and consolidation of lung in mice, providing direct evidence that hyaluronan is
342 fundamental for GGO formation. Consistent with our results, transcriptome sequencing of cells in
343 BALF from COVID-19 patients revealed differentially altered genes enriched in the hyaluronan
344 metabolic pathway¹⁹. The appearance of GGO were further interpreted by the facts that the water
345 absorption of hyaluronan can reach 1000 times its molecular weight¹⁷, possibly resulting in the
346 formation of jelly-like liquid in the lung of COVID-19 patients³. In addition to GGO, lymphopenia is
347 another typical clinical symptom in severe COVID-19 patients¹³. We found that the crucial subsets of T
348 lymphocytes, CD4+ T cells, CD8+ T cells, and CD45+ T cells were also significantly decreased in
349 COVID-19 patients with high HA. Meanwhile, the negative correlation between hyaluronan and
350 diverse T cell subsets confirmed that hyaluronan was associated with the reduction of T lymphocytes.
351 In line with this sight, hyaluronan can induce the activated T cell death by binding to its ligand CD44¹⁴.
352 Notably, CD4+ T lymphocytes become rapidly activated after SARS-CoV-2 infection²⁴, which provides
353 the condition needed for the binding of HA to CD44 located in activated T cells, leading to their death.
354 In other words, T cell exhaustion mediated by hyaluronan may potentially underly lymphopenia of
355 COVID-19 patients.

356 Hymecromone could accelerate the recovery of clinical manifestations in COVID-19 patients. At
357 present, the therapeutic strategy for COVID-19 is mainly symptomatic supportive treatment in clinic²⁵.
358 Here, we found that hymecromone inhibited hyaluronan production by suppressing the expression of
359 *HAS1/2*. Additionally, hymecromone significantly improved lymphopenia of COVID-19 patients,
360 indicating that declines in hyaluronan via hymecromone administration promote the recovery of
361 lymphopenia. Likewise, hymecromone decreased the CRP and fibrinogen elevation of COVID-19
362 patients. Also remarkably, hymecromone accelerated pulmonary lesions absorption. It has already been
363 reported that dexamethasone and metformin can significantly decrease the mortality of patients with

364 severe COVID-19²⁶⁻²⁸. Accordingly, these results may be explained by the reports that dexamethasone
365 and metformin can also rapidly decline hyaluronan synthesis by downregulating *HAS2* expression^{29,30},
366 which may contribute the therapeutic effects of these two drugs on COVID-19. In addition, we found
367 most HIS is quite conservative by analyzing 159258 genomes of SARS-CoV-2 (unpublished data),
368 suggesting hyaluronan caused by HIS may be an important therapeutic target for diverse SARS-CoV-2
369 variants. All these evidences support that hymecromone could be a potential and effective drug for
370 COVID-19 patients even infected with delta variant.

371 There are several limitations in our study. First, the total number of patients involved in our
372 clinical trial is relatively insufficient, which requires a larger sample and multi-center clinical study in
373 the future. Second, we did not evaluate whether hymecromone can reduce the mortality rates of
374 COVID-19 patients because of no critical patients in this clinical trial. Third, given that the exact value
375 of hyaluronan may be different using diverse methods, it is necessary to identify the hyaluronan
376 concentration to clinically distinguish the healthy subjects and COVID-19 patients by uniform standard
377 methods.

378 Overall, the increased hyaluronan is significantly correlated with the decreased lymphocytes and
379 pulmonary lesions of COVID-19 patients. Hymecromone administration can markedly improve the
380 clinical manifestations of COVID-19 patients. Thus, hymecromone could be a potential and efficient
381 drug for COVID-19 therapy, which is needed to further clarify the effect of hymecromone on
382 COVID-19 in a larger sample of clinical trials. Our findings highlight that inhibiting the synthesis of
383 hyaluronan with specific drugs is a promising therapeutic strategy for COVID-19.
384

385 **Contributors**

386 F.S., W.Y., and H.L. conceived and designed this study. S.Y., Y.L., F.Z., L.W., Z.S., M.L., Y.T., L. C.,
387 B.Z., , Y.S. and F.S. did the follow-up investigation. S.Y., Y.L., FZ, L.W., Q.L., D.R., T.Z., K.Z., P.X.,
388 and Z.Y. collected the data. S.Y., W.L., Q.L., and W.L. did the statistical analysis. S.Y. and F.Z. drafted
389 the initial manuscript and all the authors revised the manuscript critically. H.L. and W.Y. had full access
390 to the all data and took responsibility for the integrity and accuracy of the data in the study.

391

392 **Declaration of interests**

393 Wenqiang Yu et al are listed as inventors on patents' application related to this study. There are no other
394 relationships or activities that could influence this submitted work.

395

396 **Data sharing**

397 In this study, the personal data of patients are sensitive and can't be shared in public. However, requests
398 for data could be made to the Shanghai Public Health Clinical Center.

399

400 **Acknowledgments**

401 This work was supported by the National Key R&D Program of China (2018YFC1005004), Major
402 Special Projects of Basic Research of Shanghai Science and Technology Commission (18JC1411101),
403 Shanghai Science and Technology Innovation Action Plan, Medical Innovation Research Special
404 Project (20Z11900900). We thank Yue Yu for her editorial help and comments on the manuscript. We
405 thank Ying Guo and Cuiyun Zhu for their help on patient data collection. We thank all the participants
406 involved in this study. We also appreciate the assistance and support of Shanghai Public Health Clinical
407 Center.

408

409 **References**

- 410 1. Baj A, Novazzi F, Pasciuta R, et al. Breakthrough Infections of E484K-Harboring SARS-CoV-2
411 Delta Variant, Lombardy, Italy. *Emerg Infect Dis* 2021; **27**(12).
- 412 2. Li W, Yang S, Xu P, et al. Human Identical Sequences of SARS-CoV-2 Promote Clinical
413 Progression of COVID-19 by Upregulating Hyaluronan via NamiRNA-Enhancer Network. *BioRxiv*
414 2020: 2020.11.04.361576.
- 415 3. Xu Z, Shi L, Wang Y, et al. Pathological findings of COVID-19 associated with acute respiratory
416 distress syndrome. *The Lancet Respiratory Medicine* 2020; **8**(4): 420-2.
- 417 4. Hällgren R, Samuelsson T, Laurent TC, Modig J. Accumulation of hyaluronan (hyaluronic acid)
418 in the lung in adult respiratory distress syndrome. *Am Rev Respir Dis* 1989; **139**(3): 682-7.
- 419 5. Hellman U, Karlsson MG, Engstrom-Laurent A, et al. Presence of hyaluronan in lung alveoli in
420 severe Covid-19: An opening for new treatment options? *J Biol Chem* 2020; **295**(45): 15418-22.
- 421 6. Liang J, Jiang D, Noble PW. Hyaluronan as a therapeutic target in human diseases. *Adv Drug*
422 *Deliv Rev* 2016; **97**: 186-203.
- 423 7. Guan WJ, Ni ZY, Hu Y, et al. Clinical Characteristics of Coronavirus Disease 2019 in China. *N*
424 *Engl J Med* 2020; **382**(18): 1708-20.
- 425 8. Huang C, Wang Y, Li X, et al. Clinical features of patients infected with 2019 novel coronavirus
426 in Wuhan, China. *Lancet* 2020; **395**(10223): 497-506.
- 427 9. Nagy N, Kuipers HF, Frymoyer AR, et al. 4-methylumbelliferone treatment and hyaluronan
428 inhibition as a therapeutic strategy in inflammation, autoimmunity, and cancer. *Front Immunol* 2015; **6**:
429 123.
- 430 10. Li Q, Wang L, Wang B, Lu H. The COVID-19-designated hospitals in China: preparing for public
431 health emergencies. *Emerg Microbes Infect* 2021; **10**(1): 998-1001.
- 432 11. Shi W, Peng X, Liu T, et al. A deep learning-based quantitative computed tomography model for
433 predicting the severity of COVID-19: a retrospective study of 196 patients. *Ann Transl Med* 2021; **9**(3):
434 216.
- 435 12. Shan F, Gao Y, Wang J, et al. Abnormal lung quantification in chest CT images of COVID-19
436 patients with deep learning and its application to severity prediction. *Med Phys* 2021; **48**(4): 1633-45.
- 437 13. Richardson S, Hirsch JS, Narasimhan M, et al. Presenting Characteristics, Comorbidities, and
438 Outcomes Among 5700 Patients Hospitalized With COVID-19 in the New York City Area. *JAMA* 2020;
439 **323**(20): 2052-9.
- 440 14. Ruffell B, Johnson P. Hyaluronan induces cell death in activated T cells through CD44. *J Immunol*
441 2008; **181**(10): 7044-54.
- 442 15. Zhao W, Zhong Z, Xie X, Yu Q, Liu J. Relation Between Chest CT Findings and Clinical
443 Conditions of Coronavirus Disease (COVID-19) Pneumonia: A Multicenter Study. *AJR Am J*
444 *Roentgenol* 2020; **214**(5): 1072-7.
- 445 16. Jacobs C, van Rikxoort EM, Twellmann T, et al. Automatic detection of subsolid pulmonary
446 nodules in thoracic computed tomography images. *Med Image Anal* 2014; **18**(2): 374-84.
- 447 17. Shi Y, Wang Y, Shao C, et al. COVID-19 infection: the perspectives on immune responses. *Cell*
448 *Death Differ* 2020; **27**(5): 1451-4.
- 449 18. Kultti A, Pasonen-Seppanen S, Jauhiainen M, et al. 4-Methylumbelliferone inhibits hyaluronan
450 synthesis by depletion of cellular UDP-glucuronic acid and downregulation of hyaluronan synthase 2
451 and 3. *Exp Cell Res* 2009; **315**(11): 1914-23.
- 452 19. Andonegui-Elguera S, Taniguchi-Ponciano K, Gonzalez-Bonilla CR, et al. Molecular Alterations

- 453 Prompted by SARS-CoV-2 Infection: Induction of Hyaluronan, Glycosaminoglycan and
454 Mucopolysaccharide Metabolism. *Arch Med Res* 2020.
- 455 20. Ding M, Zhang Q, Li Q, Wu T, Huang YZ. Correlation analysis of the severity and clinical
456 prognosis of 32 cases of patients with COVID-19. *Respir Med* 2020; **167**: 105981.
- 457 21. Esposito AJ, Bhatraju PK, Stapleton RD, Wurfel MM, Mikacenic C. Hyaluronic acid is associated
458 with organ dysfunction in acute respiratory distress syndrome. *Crit Care* 2017; **21**(1): 304.
- 459 22. Ponti G, Maccaferri M, Ruini C, Tomasi A, Ozben T. Biomarkers associated with COVID-19
460 disease progression. *Crit Rev Clin Lab Sci* 2020; **57**(6): 389-99.
- 461 23. Yang S, Shi Y, Lu H, et al. Clinical and CT features of early stage patients with COVID-19: a
462 retrospective analysis of imported cases in Shanghai, China. *Eur Respir J* 2020; **55**(4).
- 463 24. Zhang W, Li L, Liu J, et al. The characteristics and predictive role of lymphocyte subsets in
464 COVID-19 patients. *Int J Infect Dis* 2020; **99**: 92-9.
- 465 25. Wiersinga WJ, Rhodes A, Cheng AC, Peacock SJ, Prescott HC. Pathophysiology, Transmission,
466 Diagnosis, and Treatment of Coronavirus Disease 2019 (COVID-19): A Review. *JAMA* 2020.
- 467 26. Group RC, Horby P, Lim WS, et al. Dexamethasone in Hospitalized Patients with Covid-19 -
468 Preliminary Report. *N Engl J Med* 2020.
- 469 27. Tomazini BM, Maia IS, Cavalcanti AB, et al. Effect of Dexamethasone on Days Alive and
470 Ventilator-Free in Patients With Moderate or Severe Acute Respiratory Distress Syndrome and
471 COVID-19: The CoDEX Randomized Clinical Trial. *JAMA* 2020; **324**(13): 1307-16.
- 472 28. Luo P, Qiu L, Liu Y, et al. Metformin Treatment Was Associated with Decreased Mortality in
473 COVID-19 Patients with Diabetes in a Retrospective Analysis. *Am J Trop Med Hyg* 2020; **103**(1):
474 69-72.
- 475 29. Gebhardt C, Averbek M, Diedenhofen N, et al. Dermal hyaluronan is rapidly reduced by topical
476 treatment with glucocorticoids. *J Invest Dermatol* 2010; **130**(1): 141-9.
- 477 30. Sainio A, Takabe P, Oikari S, et al. Metformin decreases hyaluronan synthesis by vascular smooth
478 muscle cells. *J Invest Med* 2020; **68**(2): 383-91.
- 479
480

481 **Figure Legends**

482

483 **Figure 1: The increase of hyaluronan is accompanied with the severity in COVID-19 patients**

484 (A) The plasma hyaluronan level of COVID-19 patients and normal health subjects were evaluated by
485 ELISA. The classification of mild and severe of COVID-19 was based on ground-glass opacity (GGO)
486 of chest CT. (B) ROC of the plasma hyaluronan level in normal volunteers and COVID-19 patients.
487 The 48.43 ng/ml of hyaluronan is sensitivity value to distinguish the normal subjects and COVID-19
488 patients. (D) Counts of lymphocytes upon admission plotted against hyaluronic acid. Two-tailed
489 Spearman's correlation analysis was performed to evaluate the correlation between hyaluronan and
490 lymphocyte counts. The significant difference in (A) and (C) was analyzed by the Mann-Whitney test.
491 *, $P < 0.05$; **, $P < 0.01$; ***, $P < 0.001$; ****, $P < 0.0001$; ns, not significant.

492

493 **Figure 2: The plasma level of hyaluronan as a typical indicator of COVID-19 patients in clinic**

494 C-reactive protein (A), D-dimer (C), and fibrinogen (E) of COVID-19 patients were showing based on
495 the 48.43 ng/ml of hyaluronan. Data was presented by Mean \pm SD. The significant difference was
496 confirmed by the Mann-Whitney test. *, $P < 0.05$; **, $P < 0.01$; ***, $P < 0.001$; ****, $P < 0.0001$; ns,
497 not significant. The relation of C-reactive protein (B), D-dimer (D), and fibrinogen (F) against
498 hyaluronic acid were determined by two-tailed Spearman's correlation analysis.

499

500 **Figure 3: The size of pulmonary lesions and the level of hyaluronan in one typical case**

501 (A) The plasma HA levels of this case were detected at the first day and fourth day. (B-C) The mass (B)
502 and volume (C) of pulmonary lesions including GGO and consolidation were calculated via the
503 automatic lung segmentation technology of AI based on CT images of this case at the first day and
504 fourth day. (D) Represented CT images showing the pulmonary lesions in this case. The original CT
505 results were shown in black-and-white images while the marked lesion regions of CT results were
506 shown in color images. Red regions indicated GGO, and green regions indicated consolidation.

507

508 **Figure 4: Hyaluronan directly induces GGO and consolidation in adult mice**

509 Represented CT images of lungs in mice with different treatment were shown. Adult C57BL/6 mice
510 were used to assess whether hyaluronic acid induces pulmonary lesions. We directly delivered
511 hyaluronan (200~400 kDa) to the trachea ($n = 3$), and 1 \times PBS treatment was as the control group ($n =$
512 3). Then, we monitored the lungs of mice in two groups via QuantumGX microCT at the fourth day.

513

514 **Figure 5: Hymecromone decreases hyaluronan by downregulating hyaluronic acid synthases**

515 (A) ELISA detected the hyaluronic acid of culture medium in HEK293T and HUVEC treated with
516 DMSO or hymecromone (250 μ g/ml). The fold change of hyaluronic acid was normalized to DMSO.
517 (B-C) RT-qPCR evaluated the mRNA levels of *HAS1*, *HAS2*, and *HAS3* in HEK293T (B) and
518 HEK293T treated with DMSO or hymecromone (250 μ g/ml). Data was presented by Mean \pm SD. The
519 significant difference was confirmed by unpaired t test. *, $P < 0.05$; **, $P < 0.01$; ***, $P < 0.001$; ****,
520 $P < 0.0001$; ns, not significant.

521

522 **Figure 6: The Consort Diagram and Statistical Table of recruited COVID-19 patients for this**
523 **clinical trial**

524 (A) The Consort Diagram for the clinical trial contains 144 COVID-19 patients. Among these patients,

525 94 patients were in the trial group while the rest were in the control group. Changes in lymphocytes,
526 CRP, fibrinogen, and D-dimer were set as the primary endpoints and change in chest CT results were
527 set as the secondary endpoint. (B) Statistical Table of COVID-19 patients with change in clinical
528 indicators of control group and experimental group within 35 days.

529

530 **Figure 7: Hymecromone can effectively alleviate the pulmonary lesions of severe COVID-19**
531 **patients**

532 (A) Comparison of change in chest CT results between control group and hymecromone treatment
533 group. Fisher's exact tests were used to evaluate the significance between control group and
534 experiment group. (B) Represented CT images of COVID-19 patients with support or hymecromone
535 treatment. The original CT results were shown in black-and-white images of two groups while the
536 marked lesion regions of CT results were shown in color images of two groups. Red regions indicated
537 GGO, and green regions indicated consolidation.

538

539 **Figure 8: Hymecromone accelerate the recovery of COVID-19 patients from lymphocytopenia**

540 Changes in lymphocytes (A), CRP (B), fibrinogen (C), and D-dimer (D) were calculated as the fold
541 change of diverse clinical indicators per day in patients with lymphocytopenia. Data was presented by
542 Mean \pm SD. The significant difference was confirmed by the Mann-Whitney test. *, $P < 0.05$; **, $P <$
543 0.01 ; ***, $P < 0.001$; ****, $P < 0.0001$; ns, not significant.

544

545 **Supplementary materials**

546

547 **Supplementary Figure 1: Correlation between hyaluronan and subtype of lymphocytes cell**
548 **counts in COVID-19 patients**

549 (A-C) The scatter plots showing CD4+ cell counts (A), CD8+ cell counts (B), and CD45+ cell counts
550 (C) of COVID-19 patients classified by the 48.43 ng/ml of hyaluronan. Data was expressed by Mean ±
551 SD. The significant difference was confirmed by Mann–Whitney test. *, $P < 0.05$; **, $P < 0.01$; ***, P
552 < 0.001 ; ****, $P < 0.0001$; ns, not significant. (D-F) Counts of CD4+ cells (D), CD8+ cells (E), and
553 CD45+ cells (F) upon admission plotted against hyaluronic acid, calculated by two-tailed Spearman's
554 correlation analysis.

555

556 **Supplementary Figure 2: hyaluronan and pulmonary lesions in severe COVID-19 patients**

557 (A-B) Scatter plot showing relation on the mass (A) and volume (B) of GGO against hyaluronic acid.
558 (C-D) Scatter plot showing relation on the mass (C) and volume (D) of the consolidation region against
559 hyaluronic acid. Mass and volume of pulmonary lesions were calculated via the automatic lung
560 segmentation technology of AI based on CT images of severe COVID-19 patients. GGO was defined a
561 range from -750 HU to -300 HU, and the consolidation region was defined from -300 HU to 50 HU.
562 Two-tailed Spearman's correlation analysis was performed to identify the relation of pulmonary lesions
563 against hyaluronic acid.

564

565 **Supplementary Figure 3: hymecromone helps to decrease the CRP in COVID-19 patients**

566 Changes in lymphocytes (A), CRP (B), fibrinogen (C), and D-dimer (D) were calculated as the fold
567 change of diverse clinical indicators per day in patients with CRP elevation. Data was presented by
568 Mean ± SD. The significant difference was confirmed by the Mann–Whitney test. *, $P < 0.05$; **, $P <$
569 0.01 ; ***, $P < 0.001$; ****, $P < 0.0001$; ns, not significant.

570

571 **Supplementary Figure 4: hymecromone helps to decrease fibrinogen in COVID-19 patients**

572 Changes in lymphocytes (A), CRP (B), fibrinogen (C), and D-dimer (D) were calculated as the fold
573 change of diverse clinical indicators per day in patients with fibrinogen elevation. Data was presented
574 by Mean ± SD. The significant difference was confirmed by the Mann–Whitney test. *, $P < 0.05$; **, P
575 < 0.01 ; ***, $P < 0.001$; ****, $P < 0.0001$; ns, not significant.

576

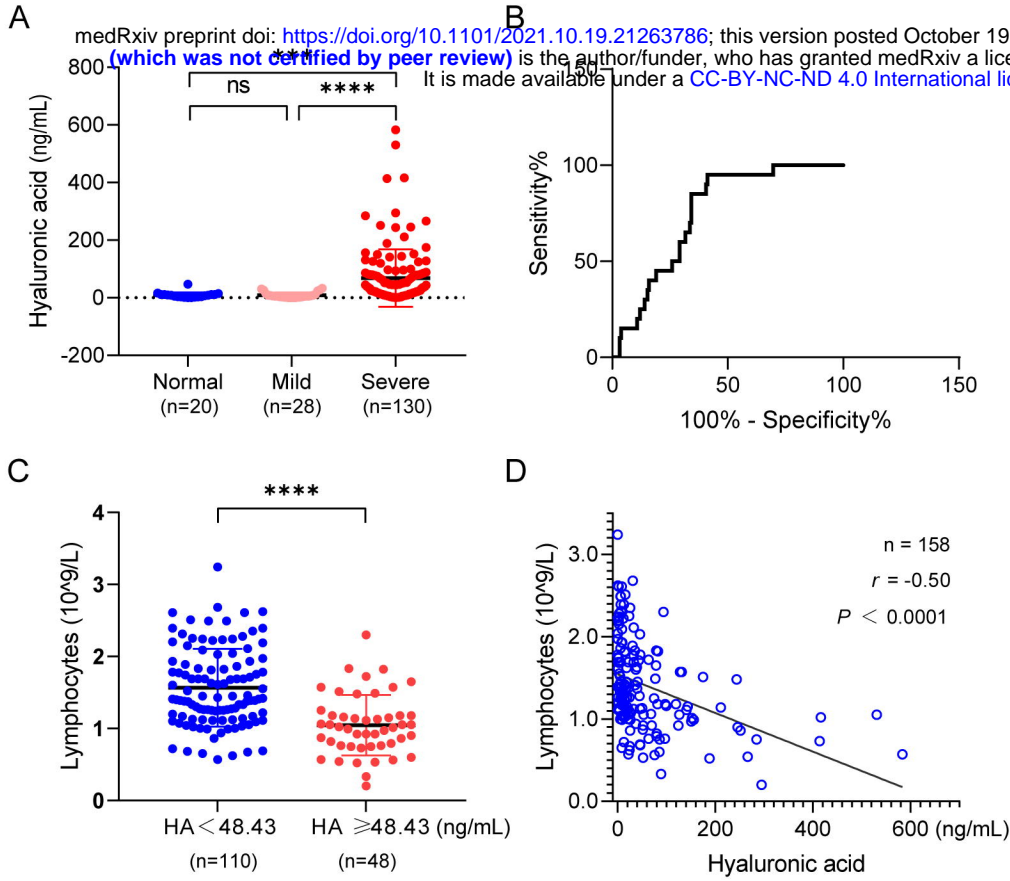
577 **Supplementary Figure 5: The effect of hymecromone on the elevation of D-dimer in COVID-19**
578 **patients**

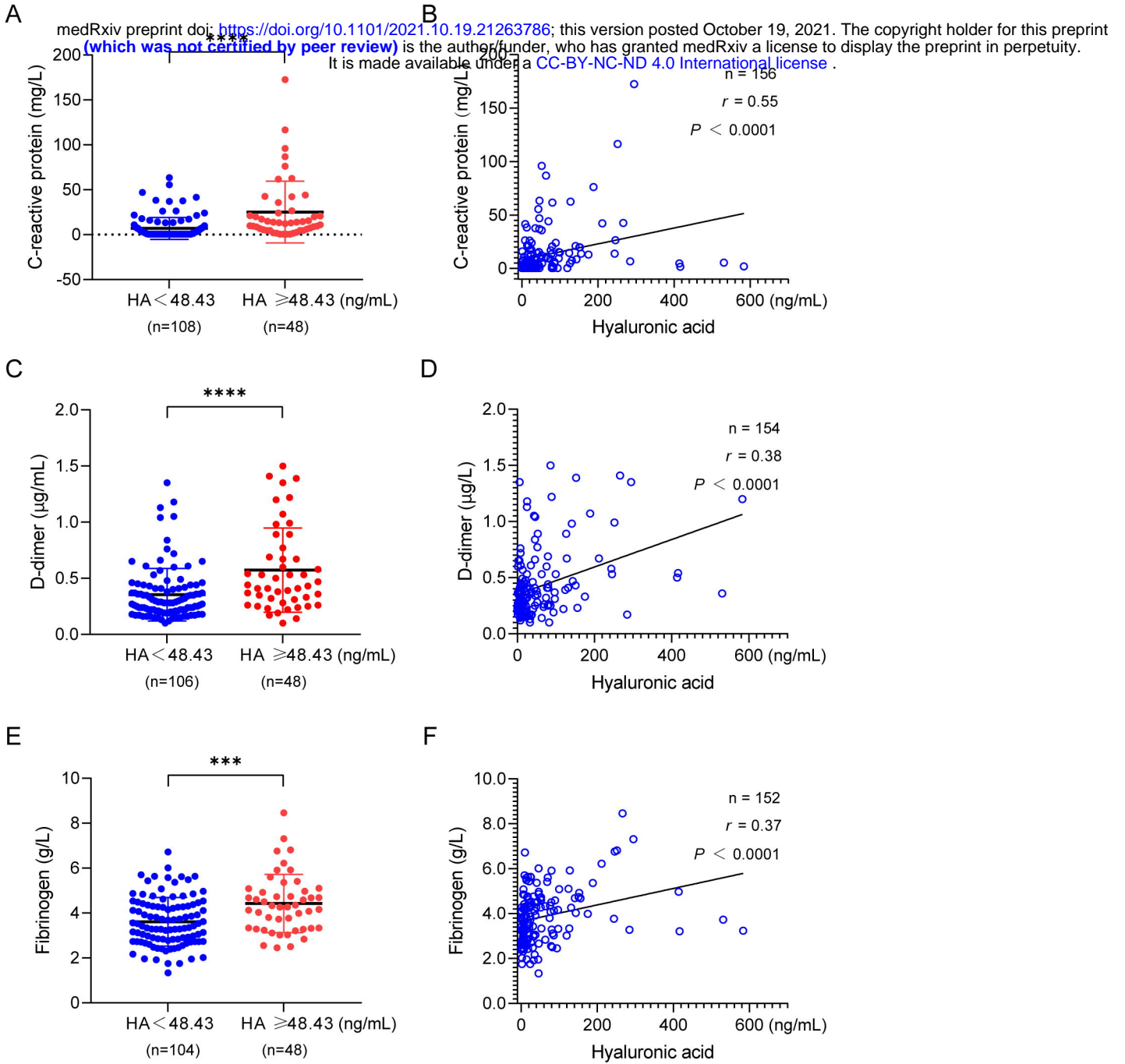
579 Changes in lymphocytes (A), CRP (B), fibrinogen (C), and D-dimer (D) were calculated as the fold
580 change of diverse clinical indicators per day in patients with D-dimer elevation. Data was presented by
581 Mean ± SD. The significant difference was confirmed by the Mann–Whitney test. *, $P < 0.05$; **, $P <$
582 0.01 ; ***, $P < 0.001$; ****, $P < 0.0001$; ns, not significant.

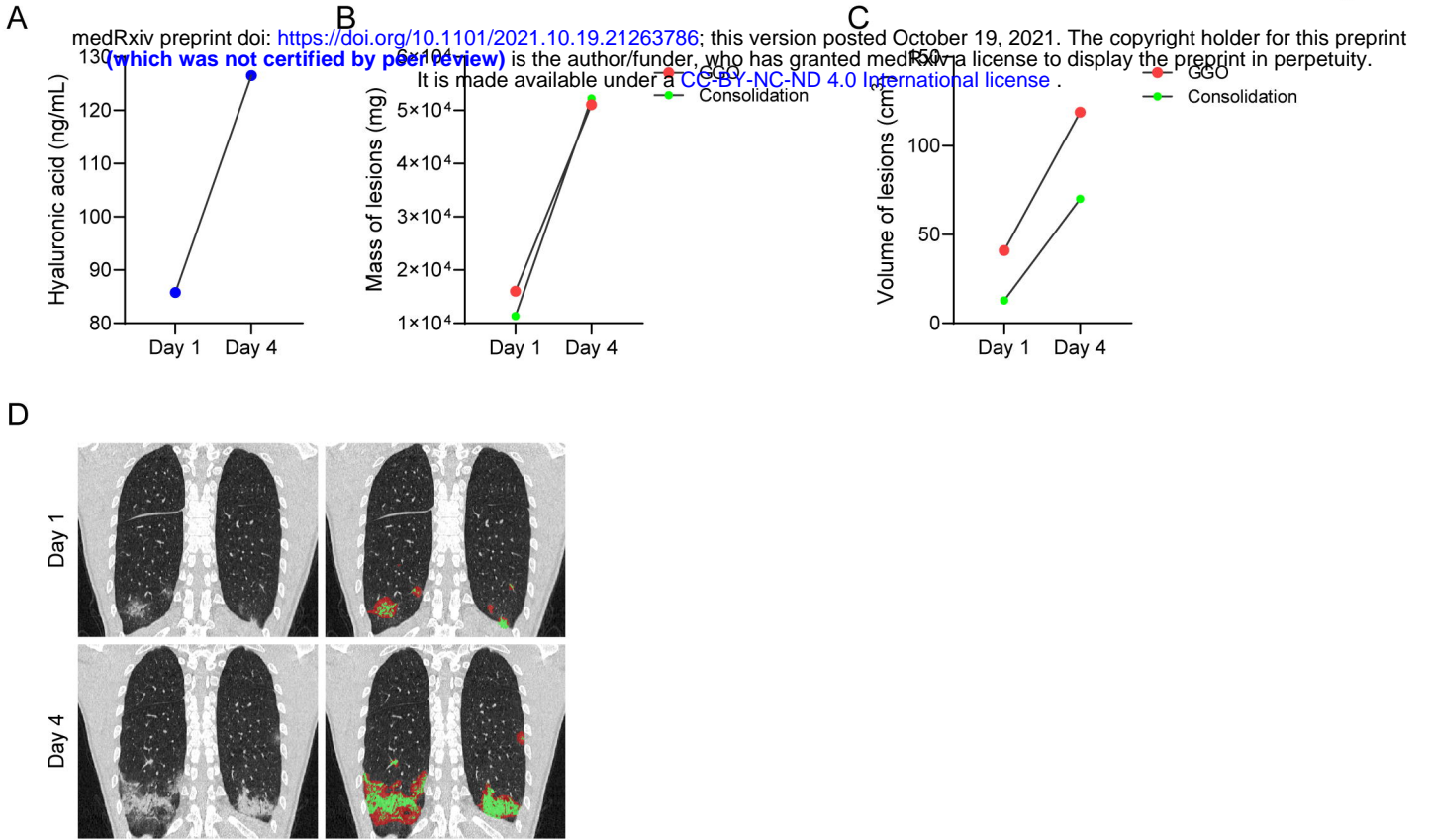
583

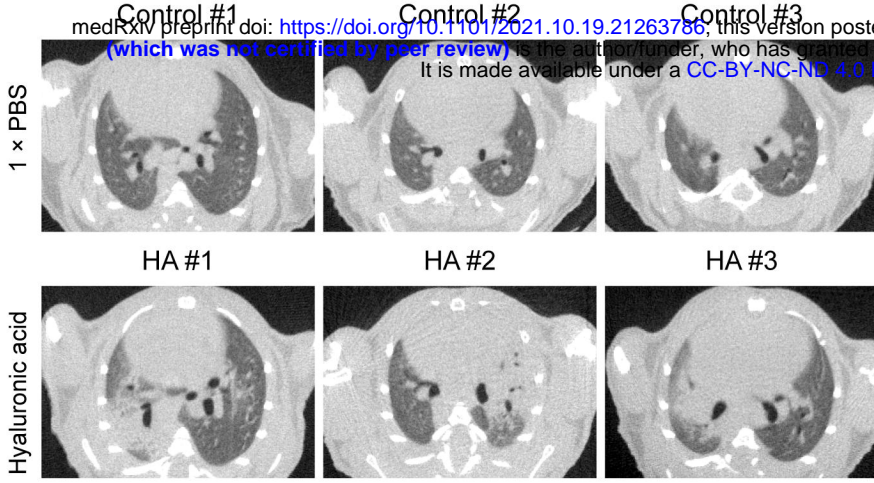
584 **Supplementary Table 1: The primer sequences for RT-qPCR.**

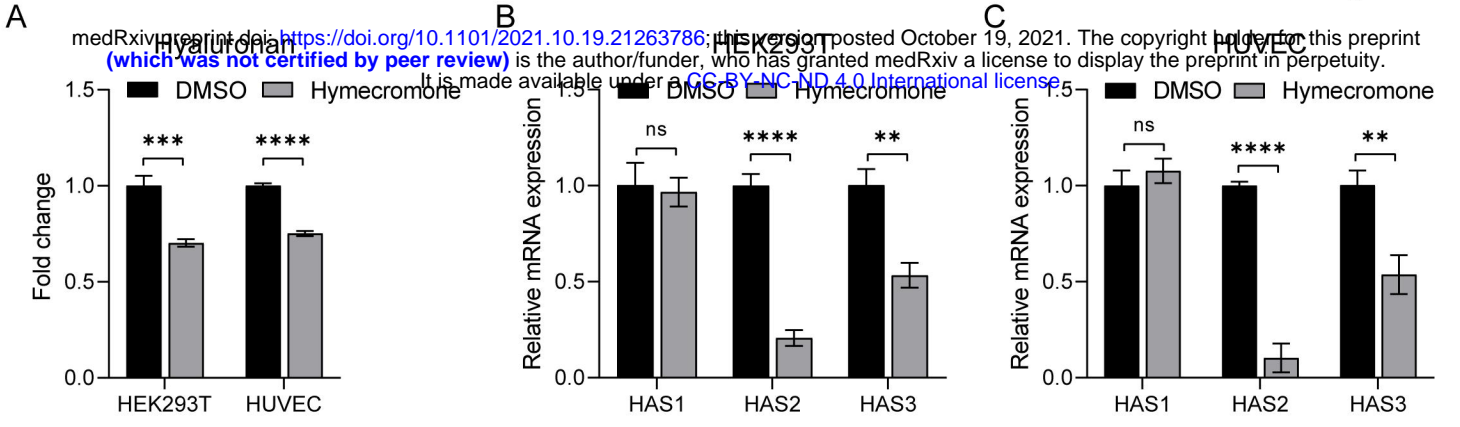
585





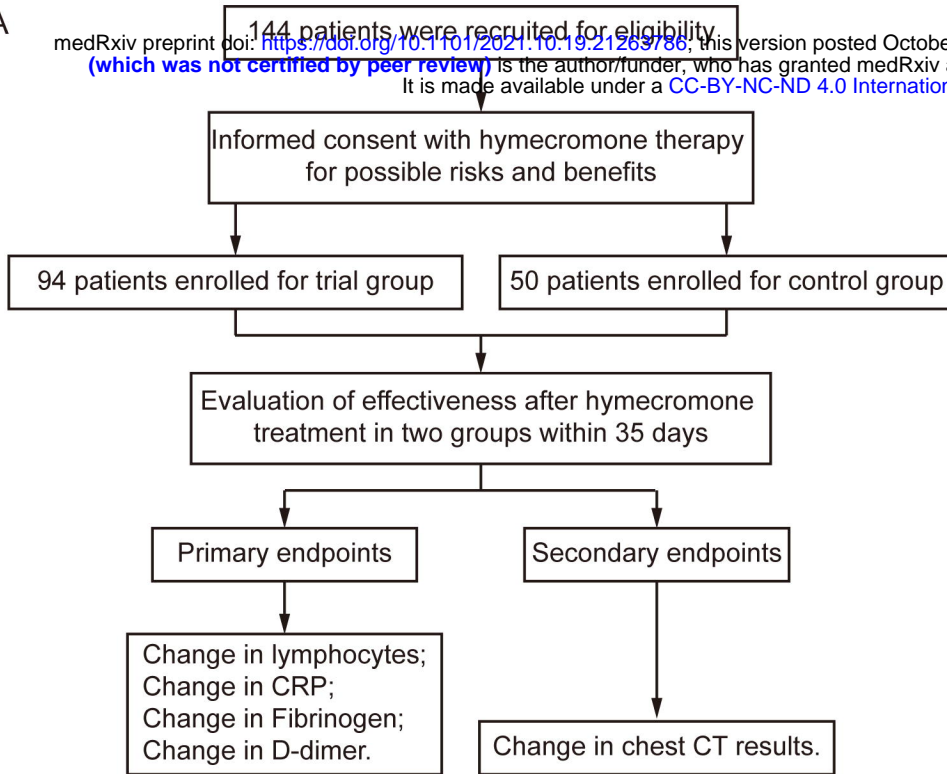






A

medRxiv preprint doi: <https://doi.org/10.1101/2021.10.19.21269786>; this version posted October 19, 2021. The copyright holder for this preprint (which was not certified by peer review) is the author/funder, who has granted medRxiv a license to display the preprint in perpetuity. It is made available under a [CC-BY-NC-ND 4.0 International license](https://creativecommons.org/licenses/by-nc-nd/4.0/).



B

Groups	Lymphopenia	CRP elevation	Fibrinogen elevation	D-dimer elevation
Control	5	4	7	8
Hymecromone	8	5	7	6

A

medRxiv preprint doi: <https://doi.org/10.1101/2021.10.19.21263786>; this version posted October 19, 2021. The copyright holder for this preprint (which was not certified by peer review) is the author/funder, who has granted medRxiv a license to display the preprint in perpetuity. It is made available under a [CC-BY-NC-ND 4.0 International license](https://creativecommons.org/licenses/by-nc-nd/4.0/).

Classification	28 day ≤ X < 35 day			Total		
	Improvement	Exacerbation	P	Improvement	Exacerbation	P
Treatment						
Control, n(%)	10 (42)	14 (58)	Yes	30 (45)	37 (55)	0.0002
Hymecromone, n(%)	11 (100)	0 (0)		24 (86)	4 (14)	
Classification	28 day ≤ X < 35 day			Total		
Treatment	Improvement	Exacerbation	P	Improvement	Exacerbation	P
Control, n(%)	2 (22)	7 (78)	0.0406	42 (42)	58 (58)	<0.0001
Hymecromone, n(%)	6 (86)	1 (14)		41 (89)	5 (11)	

B

